

Dalton Transactions

Accepted Manuscript



This is an *Accepted Manuscript*, which has been through the Royal Society of Chemistry peer review process and has been accepted for publication.

Accepted Manuscripts are published online shortly after acceptance, before technical editing, formatting and proof reading. Using this free service, authors can make their results available to the community, in citable form, before we publish the edited article. We will replace this *Accepted Manuscript* with the edited and formatted *Advance Article* as soon as it is available.

You can find more information about *Accepted Manuscripts* in the [Information for Authors](#).

Please note that technical editing may introduce minor changes to the text and/or graphics, which may alter content. The journal's standard [Terms & Conditions](#) and the [Ethical guidelines](#) still apply. In no event shall the Royal Society of Chemistry be held responsible for any errors or omissions in this *Accepted Manuscript* or any consequences arising from the use of any information it contains.

Cite this: DOI: 10.1039/c0xx00000x

www.rsc.org/xxxxxx

ARTICLE TYPE

Hemi- and holo-directed lead(II) complexes in soft ligand environment

Muhammad Imran,^a Andreas Mix,^a Beate Neumann,^a Hans-Georg Stammer,^a Uwe Monkowius,^b Petra Gründlinger^b and Norbert W. Mitzel^{a,*}

Received (in XXX, XXX) Xth XXXXXXXXX 20XX, Accepted Xth XXXXXXXXX 20XX

DOI: 10.1039/b000000x

To investigate the geometries and stereochemical activity of the lone pair at the lead atom, lead(II) complexes (**1** – **10**) with one tripodal (L^1), one dipodal (L^2) boron-centred soft ligand and eight other small soft heterocyclic ligands, 2-mercaptobenzimidazole (L^3), 2-mercapto-5-methylbenzimidazole (L^4), 3-mercapto-1,2,4-triazole (L^5 H), 3-mercapto-4-methyl-1,2,4-triazole (L^6), 2-mercapto-1,3,4-thiadiazole (L^7 H), 2-mercapto-5-methyl-1,3,4-thiadiazole (L^8 H), 5-mercapto-1-methyltetrazole (L^9 H) and 2-mercapto-4-phenylthiazole (L^{10} H) were prepared. The structures of these complexes were elucidated on the basis of X-ray crystallography, elemental analyses as well as ^1H NMR, ^1H DOSY, ^{13}C NMR and ^{207}Pb NMR spectroscopy. The coordination numbers of these complexes vary from 4 – 8. The majority of the complexes are polymeric and possess hemi-directed environments around the lead atoms. Solution studies revealed that most of the complexes are dissociated in highly polar solvents. Most of the complexes are emissive under both ambient conditions and 77 K in the solid state. However, no obvious relationship between their solid state structures and luminescence behaviour with respect to the nature of the excited state could be identified.

Introduction

Lead(II) ions have the electronic configuration $[\text{Xe}] 4f^{14}5d^{10}6s^2$ and are classified as borderline soft metal ions in the hard and soft acid base concept (HSAB) of Pearson.^{1–2} Lead is well known to be toxic for the growth of organisms and its most preferred target in organism are the sulphur rich proteins and their zinc binding sites. The replacement of zinc by lead disrupts the structures of these proteins making them dysfunctional.^{3–6}

During the last few decades, the coordination chemistry of lead(II) with hetero-donor ligands remained an active area of research due to their interesting modes of bonding. A wide range of coordination numbers (1 – 12) for Pb(II) in such complexes has been reported.^{7–11} Lead(II) complexes have not only bio-relevant importance but have also been employed as precursors for bulk or nanostructured PbS and PbSe materials.¹² It has been reported that the 6s electron pair and several other factors such as the hard or soft nature of ligands, attractive or repulsive forces etc. affect the coordination geometries about lead(II) ions.¹³ Depending on the influence of the lone pair in determining the geometries of lead(II) complexes, the terms holo- and hemi-directed have been coined.¹⁴ Despite great efforts in the past for the coordination chemistry of Pb(II) ions with S donor ligands, rational design and tuning of the ligand structure to satisfy the coordination preferences and requirements of the Pb(II) ion is still a challenging task. Our growing interest in the field of coordination chemistry of bismuth complexes with analogous sulphur donor ligands^{15,16} has prompted us to synthesize and study the coordination pattern of related lead(II) complexes with such

ligands. For this purpose, we report here the synthesis of ten lead complexes with two boron-centred and eight other small heterocyclic ligands. The presence of π -systems within these ligands may act as a chromophoric unit, which can be combined with the heavy-atom effects of lead (spin-orbit coupling) to develop cheap luminescent systems (compare for instance the efficient triplet emitter and OLED material tris(2-phenylpyridine)iridium(III)).¹⁷ Therefore, we have also investigated basic luminescent properties of some selected lead complexes within this work.

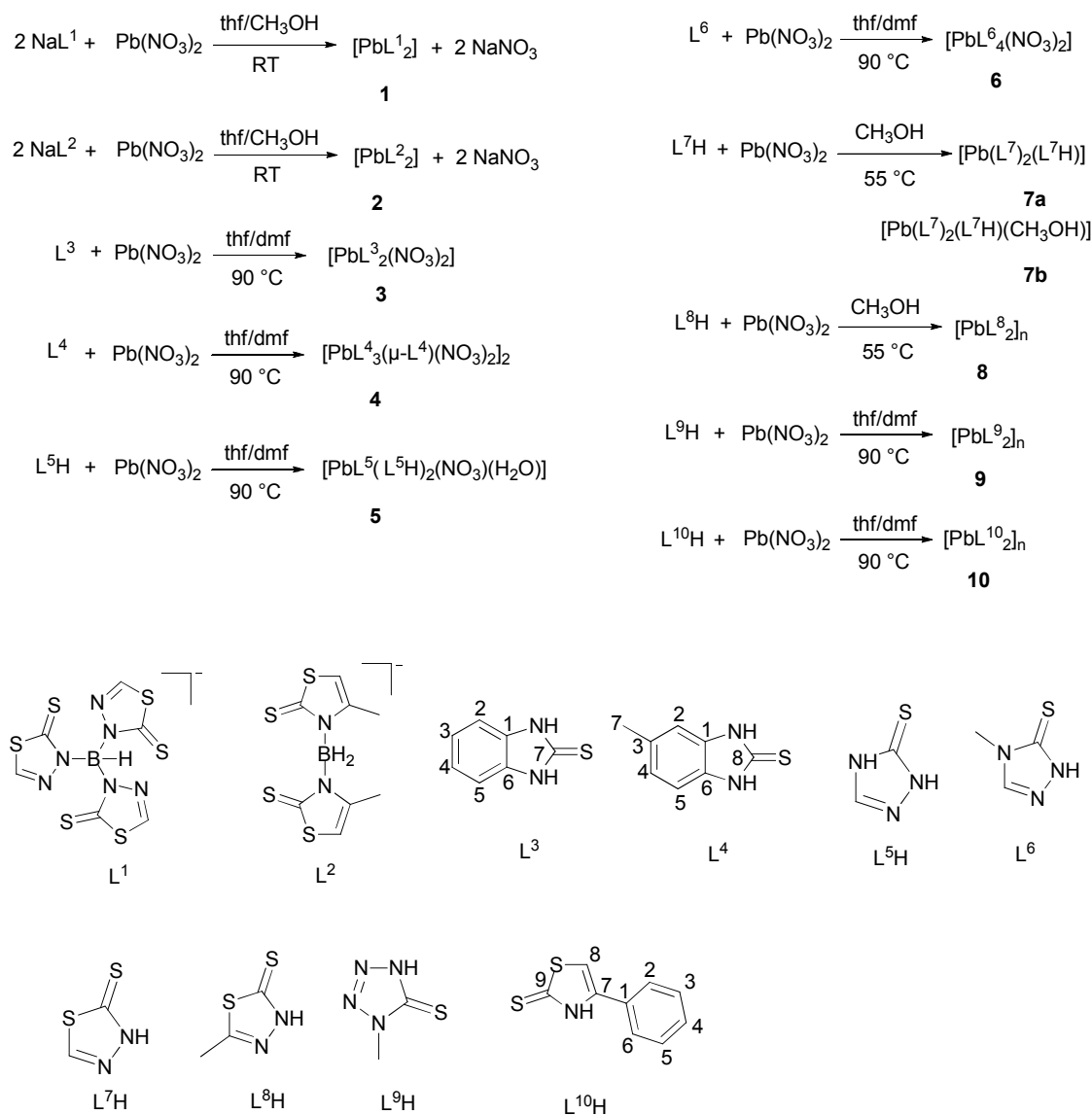
Results and discussion

Synthesis

Sodium salts of the tripodal (L^1)¹⁸ and dipodal (L^2)¹⁶ boron substituted ligands were synthesised according to literature protocols. These two ligands (L^1 , L^2) along with the other eight commercially available heterocyclic soft ligands (L^3 – L^{10} H) were reacted with lead(II) nitrate to yield lead(II) complexes (**1** – **10**) under different conditions detailed in Scheme 1. The reaction of PbNO₃ with the tripodal boron-centred soft ligand (L^1) in a 1:2 ratio afforded complex **1** as yellow precipitate which was found only to be soluble in dmf and 1-methyl pyrrolidinone. Elemental analysis data support the composition PbL¹. Crystallization of **1** was achieved by slow diffusion of *n*-pentane into a 1-methyl-2-pyrrolidinone solution resulting in yellow crystals of **1a**. In this case the free heterocycle coordinated to the lead ion is probably stemming from free-heterocycle impurities in the ligand

or its cleavage during the reaction. The majority of complexes **1** – **10** have generally poor solubility, but they are freely soluble in dmso and moderately soluble in dmf. Good yields (above 65 %)

of these complexes were obtained. Complexes **1** – **10** were characterised by ^1H NMR, ^1H DOSY NMR, ^{13}C NMR, ^{207}Pb NMR, elemental analyses and finally by single crystal X-ray diffraction.



Scheme 1. Syntheses of lead(II) complexes **1** – **10** and labelling schemes of the ligands

Solid state structures

Single crystal X-ray crystallography revealed the molecular structures of complexes **1** – **10** with compositions $[\text{Pb}(\text{L}^1)_2(\text{L}^7\text{H})_2\text{L}^1]$ **1a** (where L^1 is 1-methyl-2-pyrrolidinone), $[\text{PbL}^2_2]$ **2**, $[\text{PbL}^3_2(\text{NO}_3)_2]$ **3**, $[\text{PbL}^4_3(\mu\text{-L}^4)(\text{NO}_3)_2]$ **4**, $[\text{Pb}(\text{L}^5)(\text{L}^5\text{H})_2(\text{NO}_3)(\text{H}_2\text{O})]_n$ **5**, $[\text{PbL}^6_4(\text{NO}_3)_2]$ **6**, $[\text{Pb}(\text{L}^7)_2(\text{L}^7\text{H})]_n$ **7a**, $[\text{Pb}(\text{L}^7)_2(\text{L}^7\text{H})(\text{CH}_3\text{OH})]_n$ **7b**, $[\text{PbL}^8_2]_n$ **8**, $[\text{PbL}^9_2]_n$ **9** and $[\text{PbL}^{10}_2]_n$ **10**. Selected bond lengths and angles are presented in Tables 1 – 6 and their molecular structures are shown in Figures 1 – 10.

The molecular structure of **1a** is shown in Figure 1 and exhibits coordination number six accomplished by three sulphur atoms (S(1) from one tripodal ligand, S(3) from second tripodal ligand, S(7) from thiadiazole unit), one oxygen atom O(1) from 1-me-

thyl-2-pyrrolidinone and two nitrogen atoms (N(7) from one thiadiazole and N(8) from another thiadiazole moiety). The important bond lengths and angles are listed in Table 1 which are comparable with those of $[(\text{Tm}^{\text{Ph}})_2\text{Pb}]$,¹⁹ $[(\text{Tm}^{\text{Ph}})_2\text{Tl}]^+$,²⁰ $[(\text{Tm}^{\text{Me}})_2\text{Bi}]^+$,²¹ $[(\text{Tm}^{\text{Me}})_2\text{Tl}]^+$ ²² (where Tm = hydrotris(methyl-imazolyl)borate). The Pb–S bonds in **1a** vary between 2.843(1) and 3.095(1), and the bond angles at Pb show the stereochemical activity of the lone pair of electrons at the lead atom. In this sense the compound resembles the situation in Reglinski's $[\text{Bi}(\text{Tm})_2\text{X}]^+$ and $[\text{Bi}(\text{Tm})\text{X}(\mu\text{-X})]$ species, which both show considerable structural distortions,²³ but is in contrast $[\text{Bi}(\text{Tm})_2]^+$ which is holo-directed.²⁴

Structure **1a** can also be compared with the polymeric structure of its thallium analogue $[\{\text{HB}(\text{mtda})_3\}_2\text{Tl}]^{25}$ (where $\text{HB}(\text{mtda})_3 =$

L^1) having a TlS_6 core with octahedral geometry. The polymeric chain for **1a** is generated by a centre of inversion and translation along the crystallographic a axis.

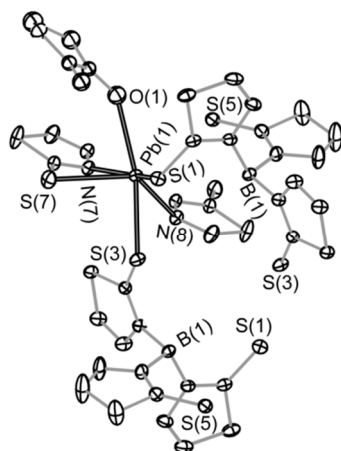


Figure 1. Molecular structure of $[Pb(L^1)_2(L^7H)_2L^1]$ **1a**. Hydrogen atoms have been omitted for clarity; displacement ellipsoids are drawn at the 50% level.

Table 1. Selected bond lengths [\AA] and angles [deg] of lead(II) complexes **1** and **2**

| | 1a | | 2 |
|-----------------|-----------|------------------|----------|
| Pb(1)–S(7) | 2.843(1) | Pb(1)–S(1) | 2.954(1) |
| Pb(1)–S(3) | 2.921(1) | Pb(1)–S(3) | 2.713(1) |
| Pb(1)–S(1) | 3.095(1) | Pb(1)–S(5) | 2.813(1) |
| Pb(1)–N(8) | 2.746(2) | Pb(1)–S(7) | 2.969(1) |
| Pb(1)–N(7) | 2.638(2) | H(1A)–Pb(1) | 2.66(2) |
| Pb(1)–O(1) | 2.674(2) | B(1)–Pb(1) | 3.609(1) |
| S(1)–C(1) | 1.687(2) | S(1)–Pb(1)–S(7) | 168.3(1) |
| S(3)–Pb(1)–S(1) | 68.9(1) | S(3)–Pb(1)–S(1) | 89.6(1) |
| S(7)–Pb(1)–S(1) | 99.8(1) | S(3)–Pb(1)–S(5) | 76.9(1) |
| S(7)–Pb(1)–S(3) | 87.5(1) | S(3)–Pb(1)–S(7) | 78.7(1) |
| N(7)–Pb(1)–N(8) | 75.6(1) | S(5)–Pb(1)–S(7) | 97.2(1) |
| N(8)–Pb(1)–S(3) | 76.4(1) | H(1A)–Pb(1)–S(5) | 128.2(5) |
| O(1)–Pb(1)–S(1) | 97.3(1) | | |
| O(1)–Pb(1)–S(3) | 159.1(1) | | |
| N(7)–Pb(1)–S(1) | 157.1(1) | | |

The molecular structure of complex **2** is shown in Figure 2 and its important bond lengths and angles are given in Table 1. In this complex the lead atom is coordinated by four sulphur atoms and a hydrogen atom of an BH_2 unit ($B(1)H(1A)\cdots Pb$ interaction). This defines one eight-membered and two six-membered rings. Overall the coordination geometry can be described as distorted octahedron with a stereochemically active lone pair. The interesting feature of the complex is the $B(1)H(1A)\cdots Pb$ interaction at a distance of 2.66(2) \AA ($Pb\cdots B(1)$ 3.609(2) \AA) by one BH_2 unit. The second distance to a BH_2 unit is $B(2)H(2A)\cdots Pb$ at 3.02 \AA but is too large to be significant. However, this BH_2 group makes a weaker contact of 2.84 \AA to a lead atom of a neighbouring molecule forming a dimer about a centre of inversion. The $B(1)H(1A)\cdots Pb$ interaction length can be compared with a related distance in $[Tl(Bt^{Me})_x]$ ($BH\cdots Tl$ distance of 2.69 \AA ($Tl\cdots B$, 3.50 \AA)).²⁶ Such interactions are characteristic features of soft borate ligands, making them flexible in binding modes and adding stabilizing effects.^{27,28}

Complex **2** when compared with its bismuth analogue $[Bi(Bt^{Me})_3]$

(where Bt^{Me} (dihydrobis(2-mercapto-4-methylthiazolyl)borate) = L^2) reported by us¹⁶ reveals significant differences. $[Bi(Bt^{Me})_3]$ is monomeric with no $BH\cdots Bi$ interaction¹⁶. To best of our knowledge, the $BH\cdots Pb$ interaction in **2** is unprecedented for complexes with dipodal boron-centred soft ligands. A similar interaction with one BH unit has been observed for the tripodal boron-centred soft-ligand lead complex $[Tm^{Ph}]_2Pb$.¹⁹

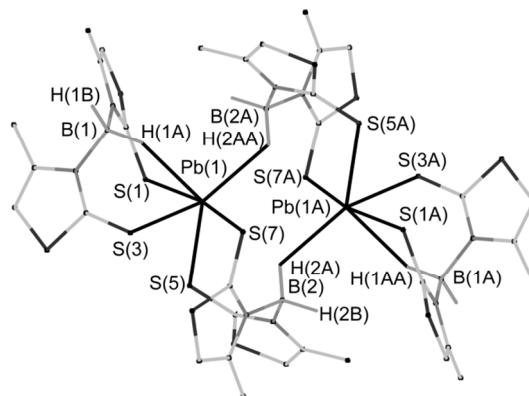


Figure 2. Solid state structure of $[PbL^2]_2$ **2**. Hydrogen atoms except bonded to boron have been omitted for clarity; displacement ellipsoids are drawn at the 50% level.

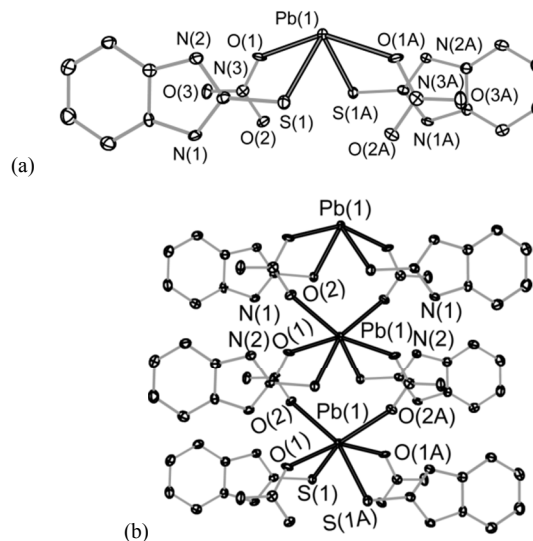


Figure 3. (a) Coordination environment around $Pb(II)$ in $[PbL^3_2(NO_3)_2]_n$ (**3**) and (b) its coordination polymer, hydrogen atoms have been omitted for clarity; displacement ellipsoids are drawn at the 50% level.

Complex **3** possesses C_2 symmetry. The lead atom is four coordinated, to two sulphur atoms of benzimidazole ligands and to two oxygen atoms of two nitrate ions, and can be referred to as hemi-directed (Figure 3a). Both, the benzimidazole and nitrate ligands, behave as monodentate. The bond lengths and angles are listed in Table 2. The interesting feature of this complex is the presence of significant secondary interactions ($Pb(1)\cdots O(2)$ 2.925(3) \AA), which are shorter than the sum of the van der Waals radii (3.10 \AA).²⁹ The hemi-directed tetrahedron (Figure 3a) with a stereochemically active lone-pair of electrons on the lead atom leaves space for bonding of an O atom of the nitrate ligand of the adjacent complex resulting in a polymeric structure along the crystallographic glide plane c (Figure 3b). Such secondary interactions

have also been reported at a distance of (Pb...O 2.989(10) Å for [Pb₂(ins)₂(CH₃CH₂OH)]_n (ins = *N*-isonicotinamidosalicylanilide dimine).²⁹ There are also weak N–H...O hydrogen-bond type intermolecular interactions where the donor-acceptor distances for N(1)–H(1)...O(1) and N(2)–H(2)...O(2) are 1.95(2) Å and 1.97(2) Å, respectively.

Complex **4** crystallizes in the monoclinic space group *C2/c*. It forms discrete dimeric units [Pb(L⁴)₃(μ-L⁴)Pb(NO₃)₂]₂ about a centre of inversion (Figure 4). The double bridging mode of sulphur is similar as the one reported for [(mimt)(NO₃)₂Pb(μ-mimt)₂Pb(NO₃)₂(mimt)₂] (where mimt = 1-methylimidazoline-2(3H)-thione).³⁰ The distances between lead and the bridging sulphur atoms are Pb(1)–S(1A) 3.098(2) Å and Pb(1)–S(1) 2.830(2) Å, while the S–Pb–S angles are Pb(1)–S(1)–Pb(1A) 102.2° and S(1)–Pb–S(1A) 77.8° resulting in a Pb...Pb distance of 4.617 Å. As expected, the Pb–S bonds to the non-bridging ligands L⁴ are shorter than those to the bridging ligands (Table 2) and are comparable with those of the discussed complex **3**. Furthermore, two mono-dentate nitrate ligands coordinate to each lead atom resulting in an overall coordination number seven.

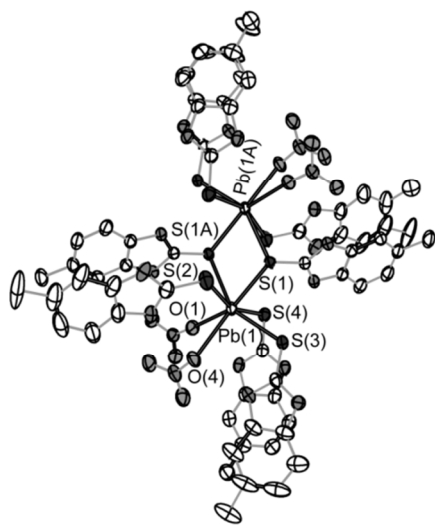


Figure 4. Solid state structure of [PbL₃(μ-L⁴)(NO₃)₂]₂ (**4**). Hydrogen atoms have been omitted for clarity, displacement ellipsoids are drawn at the 50% level.

The relatively longer Pb–O bonds (Table 2) can be compared with those in [Pb₂(phen)₂(mbtfa)₄] and in [Pb₂(dmp)₂(mbtfa)₄] (phen, dmp and mbtfa are 1,10-phenanthroline, 2,9-dimethyl-1,10-phenanthroline and 4-methoxybenzoyltrifluoroacetate,³¹ Pb–O distances: 2.829(5) – 2.918(5) Å, respectively). Note that such distances have frequently been overlooked in the past.^{32–33} Important bond angles are listed in Table 2 and the complex can be classified as hemi-directed. It is somewhat surprising for a complex with coordination number 7 to be hemi-directed, because of possible ligand crowding. However, Glusker et al.¹⁴ noticed that a relatively large number of lead(II) complexes with coordination number 7 were hemi-directed (21 out of 31 searched in the CCSD data base).

Lead complex **5** crystallizes in the form of a sheet-like structure parallel the crystallographic glide plane *b* (space group *Pbcn*, Figure 5). In this complex, each lead ion is in hemi-directed environment by coordinating one water molecule and a bidentate

nitrate ligand as well as three monodentate triazole ligands. Two of the three bind with their nitrogen sites and one through a sulphur site. The important feature of the structure is the bridging nature of S(1) that results in a sheet-like structure. The affinity of lead towards both, soft and hard donor sites, supports its borderline placement in the HSAB concept. Important bond lengths and angles of **5** are given in Table 3. They can be compared with a closely related reported structure of [Pb(trzS)]_n (where trzS = 1,2,4-triazole-3-thiol).³⁴ The latter complex was synthesised in situ by heating ahtrzSH (4-amino-3-hydrazino-5-mercapto-1,2,4-triazole) and possesses a square pyramidal environment (N₃S₂) with coordination number 5.

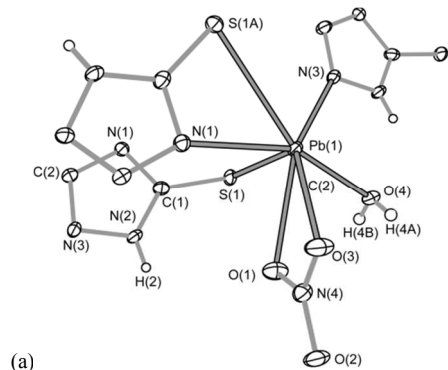
Table 2. Selected bond lengths [Å] and angles [deg] of complexes **3** and **4**

| 3 | | 4 | |
|------------------|----------|-----------------|----------|
| Pb(1)–S(1) | 2.886(1) | Pb(1)–S(1) | 2.830(1) |
| Pb(1)–S(1A) | 2.886(1) | Pb(1)–S(1A) | 3.098(1) |
| Pb(1)–O(1) | 2.574(3) | Pb(1)–S(3) | 2.859(1) |
| Pb(1)–O(1A) | 2.574(3) | Pb(1)–S(2) | 2.953(1) |
| Pb(1)–O(2) | 2.925(3) | Pb(1)–S(4) | 2.985(1) |
| Pb(1)–O(2A) | 2.925(3) | Pb(1)–O(4) | 2.887(3) |
| N(1)–H(1)...O(1) | 1.95(2) | Pb(1)–O(1) | 2.938(2) |
| S(1)–C(1) | 1.719(5) | S(1)–Pb(1)–S(3) | 76.5(1) |
| O(1)–Pb(1)–S(1) | 78.1(1) | S(1)–Pb(1)–S(2) | 67.9(1) |
| O(1)–Pb(1)–O(1A) | 147.9(1) | S(3)–Pb(1)–S(2) | 99.7(1) |
| S(1)–Pb(1)–S(1A) | 95.4(1) | S(3)–Pb(1)–S(4) | 81.4(1) |
| | | S(2)–Pb(1)–S(4) | 160.2(1) |
| | | S(3)–Pb(1)–S(1) | 148.9(1) |
| | | S(2)–Pb(1)–S(1) | 86.5(1) |
| | | S(4)–Pb(1)–S(1) | 83.0(1) |

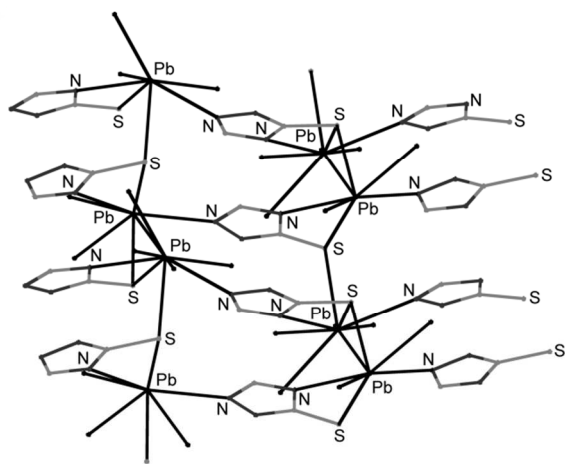
Table 3. Selected bond lengths [Å] and angles [deg] of complexes **5** and **6**

| 5 | | 6 | |
|------------------|----------|------------------------|----------|
| Pb(1)–S(1) | 2.817(1) | Pb–S | 3.020(1) |
| Pb(1)–S(1A) | 3.131(1) | Pb–O | 2.726(2) |
| Pb(1)–N(1) | 2.540(4) | S(1)–C(1) | 1.694(3) |
| Pb(1)–N(3) | 2.764(4) | O–Pb(1)–O <i>cis</i> | 46.8(1) |
| Pb(1)–O(1) | 2.632(3) | O–Pb–O <i>trans</i> | 147.4(1) |
| Pb(1)–O(3) | 2.856(3) | S–Pb(1)–S <i>trans</i> | 153.4(1) |
| Pb(1)–O(4) | 2.716(3) | S–Pb(1)–S <i>cis</i> | 93.0(1) |
| O(1)–Pb(1)–S(1) | 76.2(1) | | |
| O(4)–Pb(1)–S(1) | 77.1(1) | | |
| O(1)–Pb(1)–O(4) | 75.9(1) | | |
| N(1A)–Pb(1)–S(1) | 83.0(1) | | |
| N(3)–Pb(1)–S(1) | 77.8(1) | | |
| O(1)–Pb(1)–N(3) | 138.7(1) | | |
| O(3)–Pb(1)–S(1) | 121.5(1) | | |
| O(3)–Pb(1)–O(4) | 95.6(1) | | |

Complex **6** was synthesised using a methyl substituted 1,2,4-triazole under similar conditions as for complex **5**. The solid-state structure of **6** reveals a remarkable contrast to **5** and is monomeric with coordination number 8 and *S*₄ symmetry. The Pb atom is coordinated by four 3-mercapto-4-methyl-1,2,4-triazole (L⁶) ligands via their sulphur donor atoms and by two bidentate nitrate ligands (Figure 6). The Pb–S and Pb–O bond lengths are 3.020(2) Å and 2.726(2) Å, respectively. Complex **6** is holo-directed in contrast to **5**. Glusker et al.¹⁴ have found the majority of lead(II) complexes in the CCSD database with coordination number 8 to be holo-directed.



(a)



(b)

Figure 5. (a) Coordination environment around the Pb ion of $[\text{Pb}(\text{L}^5)(\text{L}^7\text{H})_2(\text{NO}_3)(\text{H}_2\text{O})]_n$ **5**, (b) part of sheet like structure of $[\text{Pb}(\text{L}^5)(\text{L}^7\text{H})_2(\text{NO}_3)(\text{H}_2\text{O})]_n$ **5**. Hydrogen atoms have been omitted for clarity, displacement ellipsoids are drawn at the 50% level.

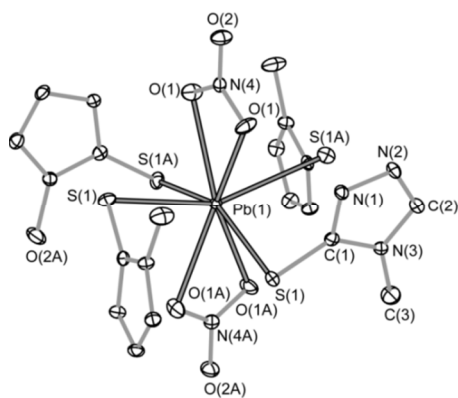
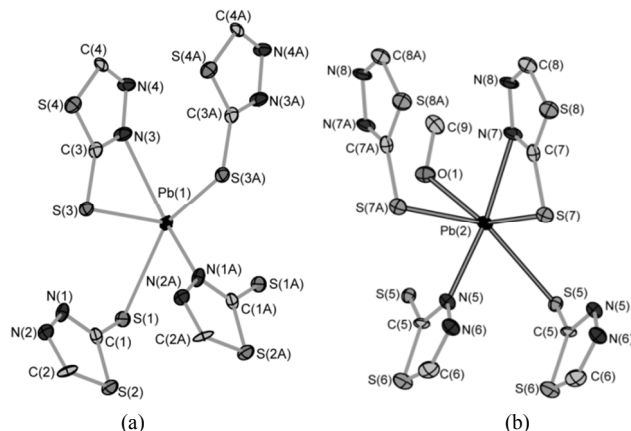


Figure 6. Solid state structure of $[\text{PbL}^6_4(\text{NO}_3)_2]$ (**6**). Hydrogen atoms have been omitted for clarity, displacement ellipsoids are drawn at the 50% level.

Figure 7 shows the molecular structure of complex **7**. In the solid state this complex comprises two 1D coordination polymers **a** and **b**. The two coordination polymers are linked through S(5) and run along the *a* axis. The two ligands (L^7H) at each Pb atom in both molecules **a** and **b** have different coordination modes (Figures 7a and 7b). For example, in molecule **a**, one of the ligand (L^7H) behaves bidentate and coordinates via S(3) [Pb(1)–S(3) 2.852(3) Å] and N(3) [Pb(1)–N(3) 2.864(13) Å] donor atoms. However, S(3) is bridging and coordinates further to the next lead atom at a distance of Pb(1)–S(3) 3.016(3) Å. The second hetero-

cyclic ligand (L^7H) coordinates to Pb(1) only via N(1) (Pb(1)–N(1) 2.534(9) Å) and uses its S(1) donor site to coordinate to a lead atom of the neighbouring monomeric unit (Figure 7c). The coordination number around each lead ion of **a** is five with a distorted square pyramidal geometry. The presence of a stereochemically active lone pair is manifest from a void as well as the distribution of bond angles (Table 4). In the polymer chain of **b** (Figure 7d), the coordination number at each lead ion is six with an additional Pb–O bond to a methanol solvent molecule. Important bond lengths and angles are listed in Table 4; they are slightly different from those of molecule **a**. Another difference between the two molecules **a** and **b** is that **a** has only one bridging atom, S(3), while **b** has two, S(7) and O(1).



35

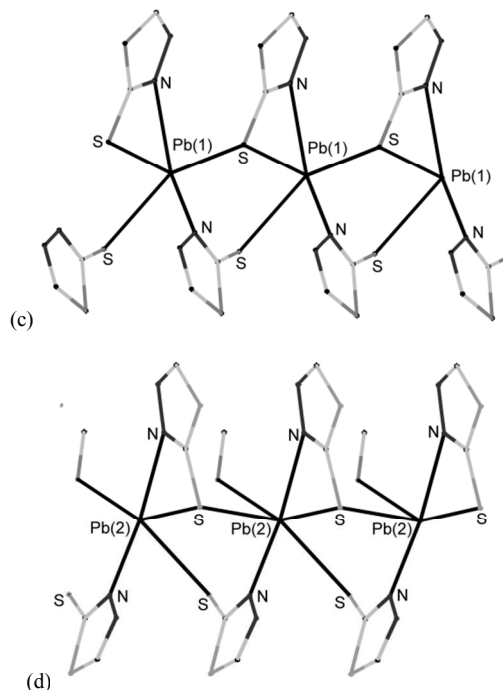


Figure 7. (a) Monomeric unit of $[\text{Pb}(\text{L}^7)_2(\text{L}^7\text{H})]_n$ **7a**, (b) monomeric unit of $[\text{Pb}(\text{L}^7)_2(\text{L}^7\text{H})(\text{CH}_3\text{OH})]_n$ **7b**, (c) part of polymeric structure of $[\text{Pb}(\text{L}^7)_2(\text{L}^7\text{H})]_n$ **7a**, (d) part of polymeric structure of $[\text{Pb}(\text{L}^7)_2(\text{L}^7\text{H})(\text{CH}_3\text{OH})]_n$ **7b**. Hydrogen atoms have been omitted for clarity, displacement ellipsoids are drawn at the 50% level.

X-ray diffraction analysis for complex **8** shows it to possess a polymeric structure assembled via the S(1) atom. This bridges two lead ions in the chain (Figure 8). The coordination geometry

of each lead atom in this polymeric chain (running along the crystallographic c axis, space group $P2_1/c$) is irregular five-coordinated with a hemi-directed environment and can be best described as distorted square pyramidal. Selected bond lengths and angles are listed in Table 4. They are similar to those of complex **5** discussed above as well as with the reported structure of $[\text{Pb}(\text{trzS})]_n$ (where $\text{trzS} = 1,2,4\text{-triazole-3-thiole}$).³⁴

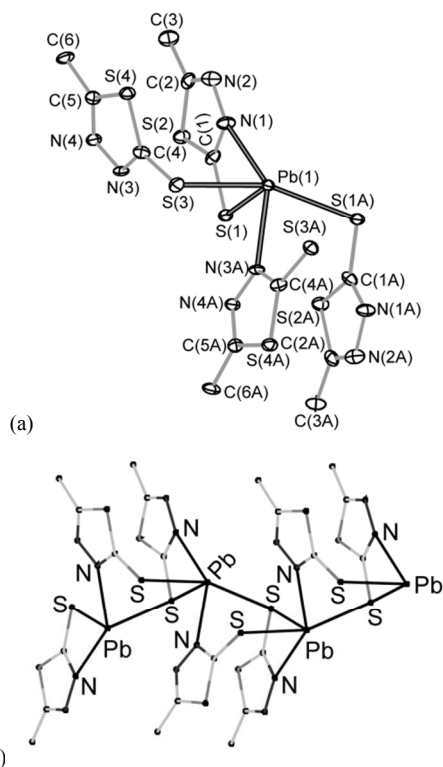


Figure 8. (a) Monomeric unit of $[\text{PbL}^8]_n$ **8** (b) part of polymeric structure of $[\text{PbL}^8]_n$ **8**. Hydrogen atoms have been omitted for clarity, displacement ellipsoids are drawn at the 50% level.

In complex **9** each Pb(II) ion is five-coordinate (similar to complex **8**) by three sulphur and two nitrogen atoms from three tetrazole ligands (L^9H) forming a distorted square pyramidal coordination geometry (Figure 9). One tetrazole ligand (L^9H) acts as bridging bidentate via its N(4) and S(1) sites forming a chain along the crystallographic two-fold screw axis along b , whereas the second (L^9H) acts as tridentate via N(8) and S(2). S(2) makes a bridge to the lead atom Pb(1A) of the second chain, thereby forming a double chain (running along axis b). Bond lengths and angles (Table 5) are similar to those in related lead complexes based on differently substituted tetrazole ligands.^{35–36}

Table 4. Selected bond lengths [Å] and angles [deg] of complexes **7a** and **7b**

| 7a | | 7b | |
|------------------|-----------|-------------------|-----------|
| Pb(1)–S(3) | 2.852(3) | Pb(2)–S(7) | 2.847(3) |
| Pb(1)–S(3A) | 3.016(3) | Pb(2)–S(7A) | 2.950(3) |
| Pb(1)–S(1) | 3.086(3) | Pb(2)–S(5) | 3.058(3) |
| Pb(1)–N(1) | 2.534(9) | Pb(2)–N(7) | 2.791(9) |
| Pb(1)–N(3) | 2.864(13) | Pb(2)–N(5) | 2.595(9) |
| N(1)–Pb(1)–S(3) | 88.5(2) | Pb(2)–O(1) | 2.865(12) |
| N(1)–Pb(1)–S(3A) | 65.7(2) | Pb(2)–O(1A) | 2.943(12) |
| S(3)–Pb(1)–S(3) | 87.3(1) | N(5)–Pb(2)–N(7) | 133.2(3) |
| N(1)–Pb(1)–S(1) | 77.5(2) | N(5)–Pb(2)–S(7) | 88.5(2) |
| S(3)–Pb(1)–S(1) | 86.6(1) | N(7)–Pb(2)–S(7) | 56.8(2) |
| N(1)–Pb(1)–N(3) | 126.8(4) | N(5)–Pb(2)–S(7A) | 65.7(2) |
| | | N(7)–Pb(2)–S(7A) | 81.7(2) |
| | | S(7)–Pb(2)–S(7A) | 88.6(1) |
| | | N(7)–Pb(2)–S(5A) | 125.0(2) |
| | | Pb(2)–O(1)–Pb(2A) | 88.4(3) |
| | | Pb(2)–S(7)–Pb(2A) | 88.7(1) |

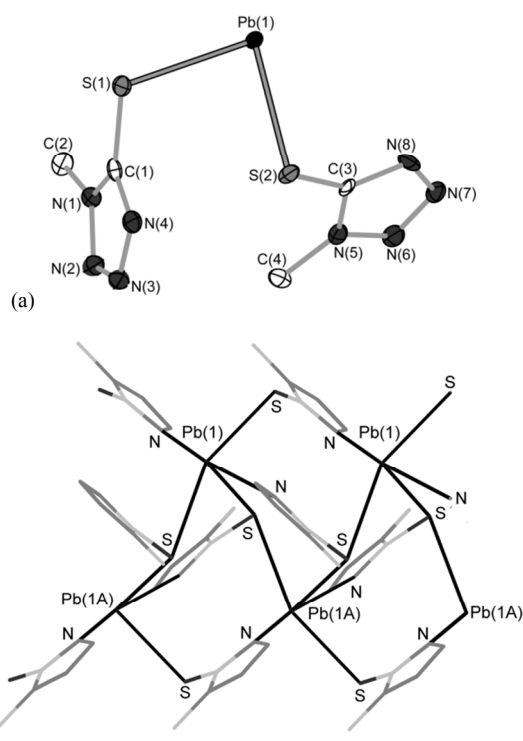


Figure 9. (a) Asymmetric unit of $[\text{PbL}^9]_n$ **9** with labelling of all atoms for clarity, (b) part of double chain of $[\text{PbL}^9]_n$ **9**. Hydrogen atoms have been omitted for clarity, displacement ellipsoids are drawn at the 50% level.

Table 5. Selected bond lengths [Å] and angles [deg] of complex **8**

| | |
|------------------|----------|
| Pb(1)–S(1) | 2.778(3) |
| Pb(1)–S(1A) | 2.993(3) |
| Pb(1)–S(3) | 2.922(3) |
| Pb(1)–N(3) | 2.473(8) |
| Pb(1)–N(1) | 2.827(9) |
| S(3)–Pb(1)–S(1) | 91.0(1) |
| S(1)–Pb(1)–S(1A) | 84.3(1) |
| N(1)–Pb(1)–N(3) | 131.1(3) |
| N(3)–Pb(1)–S(1A) | 81.3(2) |
| N(3)–Pb(1)–S(1) | 76.5(2) |
| N(3)–Pb(1)–S(3) | 79.8(2) |
| N(1)–Pb(1)–S(3) | 86.4(2) |

Lead complex **10** with 2-mercapto-4-phenylthiazole ($L^{10}H$) exhibits a polymeric structure (running along glide plane b of $Pbca$) (Figure 10). Each lead atom adopts a distorted octahedral geometry with hemi-directed environment defined by four sulphur and two nitrogen atoms of 2-mercapto-4-phenylthiazole ($L^{10}H$). Both ligands ($L^{10}H$) chelate the lead(II) ion and the sulphur atoms form bridges. Bond lengths and angles are listed in Table 6. The Pb–S distances are similar to those observed for complex **4** and can also be compared with those of $[(mimt)(NO_3)_2Pb(\mu-mimt)_2Pb_2(NO_3)_2(mimt)_2]$ ($mimt = 1\text{-methylimidazole-}2(3H)\text{-thione}$).³⁰

Table 6. Selected bond lengths [Å] and angles [deg] of complexes **9** and **10**

| 9 | | 10 | |
|--------------------|-----------|-------------------|----------|
| Pb(1)–S(1) | 2.810 (2) | Pb(1)–S(1) | 2.788(1) |
| Pb(1)–S(2A) | 3.108(2) | Pb(1)–S(1A) | 3.097(1) |
| Pb(1)–S(2) | 2.745(2) | Pb(1)–S(3) | 2.818(1) |
| Pb(1)–N(8) | 2.749(7) | Pb(1)–S(3A) | 2.980(1) |
| Pb(1)–N(4) | 2.589(8) | Pb(1)–N(1) | 2.742(3) |
| S(1)–Pb(1)–S(2) | 154.2(1) | Pb(1)–N(2) | 2.731(3) |
| S(1)–Pb(1)–S(2A) | 84.9(1) | S(1)–Pb(1)–S(3) | 87.0(1) |
| S(2)–Pb(1)–S(2A) | 86.3(1) | S(1)–Pb(1)–S(3A) | 87.3(1) |
| N(8)–Pb(1)–N(4) | 163.2(2) | S(1A)–Pb(1)–S(3A) | 173.5(1) |
| N(8)–Pb(1)–S(2A) | 82.8(2) | S(1)–Pb(1)–N(1) | 58.2(1) |
| Pb(1)–S(2)–Pb(1A) | 114.1(1) | S(3)–Pb(1)–N(2) | 57.8(1) |
| Pb(1)–S(2A)–Pb(1A) | 114.1(1) | N(2)–Pb(1)–N(1) | 155.4(1) |
| | | Pb(1)–S(1A)–Pb(1) | 92.8(1) |
| | | Pb(1)–S(3A)–Pb(1) | 94.8(1) |

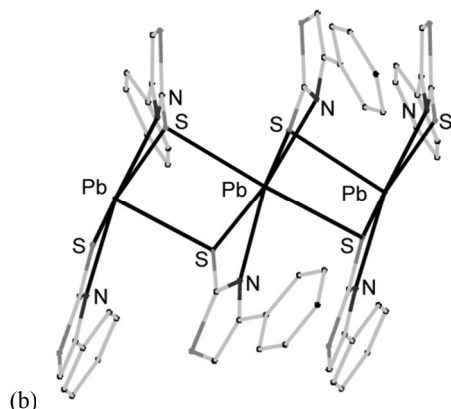
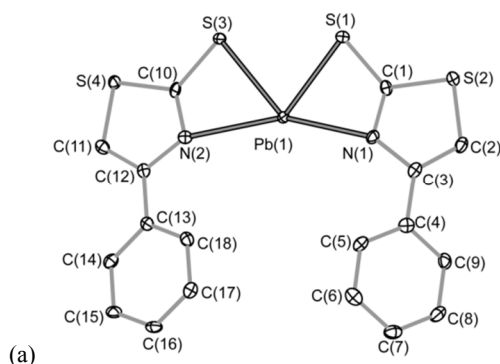


Figure 10. (a) Asymmetric unit of $[PbL^{10}_2]$ (**10**) with labelling of all atoms for clarity, (b) part of extended structure of $[PbL^{10}_2]_n$ (**10**). Hydrogen atoms have been omitted for clarity, displacement ellipsoids are drawn at the 50% level.

Solution studies

1H NMR spectra of the complexes were recorded in $dmf-d_7$ and $dmsd-d_6$ depending on the solubility of the respective complex (see experimental section). The 1H NMR and ^{13}C NMR spectra of complexes (**1** – **10**) were compared with those of the free ligand compounds (L^1 – $L^{10}H$). 1H NMR spectra of complexes **1**, **3**, **4**, **6** and **7** show slight variations in chemical shifts when compared with those of the respective free ligand compounds, indicating a significant dissociation of these complexes. However, for complexes **2**, **5**, **8**, **9** and **10** the protons of the C_6H_5 , CH_3 and CH groups exhibit a notable chemical shift (see experimental section). For example, the 1H NMR spectrum of complex **2** exhibits two signals at 6.34 and 2.13 ppm for the HC-ring and CH_3 protons, respectively, but at 6.22 (HC-ring) and 2.37 ppm (CH_3) for the free ligand compound L^2 . Moreover, in this spectrum no BH_2 signals were observed at room temperature; a similar observation has been reported.³⁷ Interestingly, in the ^{11}B NMR of this complex two different signals at -14.25 ppm and -1.96 ppm were observed indicating different environments of B atoms (Figure 11). This might be due to the monomeric nature of the complex in solution staying in interaction with only one BH unit (the stronger one at a distance of 2.66 Å). However, in complex **1** no such interaction can be established.

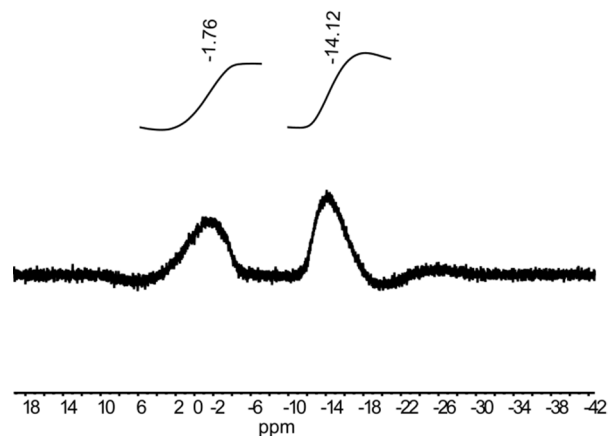


Figure 11. ^{11}B NMR spectrum of complex **2**

The ^{13}C NMR chemical shifts of the complexes **1**, **3**, **4**, **6**, **7** and **8** are very similar to those of the corresponding free ligands, supporting the interpretation in terms of dissociation. However, the ^{13}C NMR spectra of **2**, **5**, **9** and **10** show significant chemical shifts differences for carbon signals compared to their ligand compounds. The most important feature of these ^{13}C NMR spectra is the up-field shift (ca. 4 – 15 ppm, see experimental section) of the $C=S$ units in these complexes indicating thione-sulphur coordination.

In order to investigate the dissociation behaviour of these complexes in polar solvents, diffusion NMR experiments have been performed exemplarily for **2**, **3** and **6**. The diffusion coefficients of **3** and **6** (see Table 7) do not differ significantly from those of the respective ligand compounds. This indicates **3** and **6** to be dissociated to a large extent. However, the diffusion coefficient of **2** is significantly smaller than that of the corresponding ligand compound. This indicates that in DMSO a considerable part of **2** is not dissociated, as can also be concluded from the 1H NMR data.

For the majority of the complexes no ^{207}Pb NMR signals could be recorded at room temperature or, as found for **2**, **7**, **8** and **9**, they exhibit broad signals with poor signal-to-noise ratios and variations in chemical shifts indicating the presence of an equilibrium of different exchanging species in solution. This has been proven by an NMR experiment in which the ^{207}Pb resonance of a solution of lead(II) nitrate in dmsO disappears immediately when the ligand compound in 1:2 ratio was added.

Table 7. Diffusion co-efficient of complexes **2**, **3** and **6**

| Compound | Diffusion co-efficient (m^2s^{-1}) |
|------------------|--|
| 2 | CH ($2.34 \cdot 10^{-10}$) |
| FLC (2) | CH ($2.62 \cdot 10^{-10}$) |
| 3 | C_6H_5 ($2.79 \cdot 10^{-10}$) |
| FLC (3) | C_6H_5 ($2.83 \cdot 10^{-10}$) |
| 6 | CH ($3.44 \cdot 10^{-10}$) |
| FLC (6) | CH ($3.59 \cdot 10^{-10}$) |

where FLC is the free ligand compound of respective complex

Photophysical studies

In previous publications we reported on basic luminescence properties of bismuth(III) complexes bearing the same or similar ligands as presented here. In general, we found that bismuth(III) complexes are poor emitters which can be rationalised by several reasons: (i) Exciting an s^2 -ion leads to a considerable structural change in the excited state. This process can result in an efficient vibronic (i.e. non-radiative) relaxation of the excited state. (ii) The frontier orbitals, i.e. the ‘highest’ HOMOs and ‘lowest’ LUMOs are each very close in energy which makes it difficult to tune the emission properties by straightforward ligand modifications.³⁸ Indeed, we observed a considerable change of the nature of the luminescence properties by just small alteration of the coordination environment.^{15,16} Therefore, it is difficult to predict whether a complex will be emissive or not. (iii) Bond energies between heavy s^2 -elements and coordinating atoms, e.g. M–C bonds, are often very weak and therefore prone to photolytic cleavage. Therefore, excitation might not lead to an emission but to a permanent photoproduct – often to the elemental metal and organic coupling or oxidation products.^{39,40} All mentioned processes significantly reduce the emission quantum yields or even prohibit luminescence under ambient conditions, particularly in solutions. As these processes are reduced at low temperature, the luminescence intensities can be significantly enhanced under cryoscopic conditions.

Due to identical s^2 -electron configuration, we expected a comparable emission behaviour also for lead(II). However, a series of intensive luminescent Pb(II) complexes has been reported previously.^{39,41,42} Neglecting the hemi- and holo-coordination geometry around the lead ions, the principle coordination environments are similar for all complexes with a sulphur substituted N-heterocycle bonding via its S atom to the Pb atom. Hence, the following transitions are theoretically feasible: (i) a sp metal centred transition (MC); (ii) a ligand-to-metal charge transfer from the S to the Pb atom (LMCT); (iii) a π - π^* intra-ligand transition (IL). However, we found a diverse emission behaviour, which makes it difficult to rationalize the luminescence behaviour in terms of structure-property relationships.

In solution, the composition of the complexes is partly ambiguous due to dissociation equilibria (see above). With the exception of **5** and **9**, the UV-vis spectra of the ligands and complexes are almost identical. This supports the NMR investigation which reveals that in **5** and **9** the ligands are still coordinated to the metal ion. For the other complexes the dominant absorbing component is the free ligand. Therefore and also due to the poor solubility of the complexes in ‘standard’ spectroscopic solvents, we will focus on the luminescence properties in solid-state where the composition and structure are known.

Contrary to the bismuth compounds, most complexes are emissive both at r.t. and 77 K in the solid state (exception **2** and **10**). In general, we observed two different shapes of luminescence bands shining light on the possible nature of the excited states: (i) a structured band at high energy (HE) or low energy (LE), which is indicative for an IL excited state; (ii) a broad LE band with a huge Stokes shift, particular observed at 77 K. Here, a sp-transition or a LMCT or a mixture of both is possible.

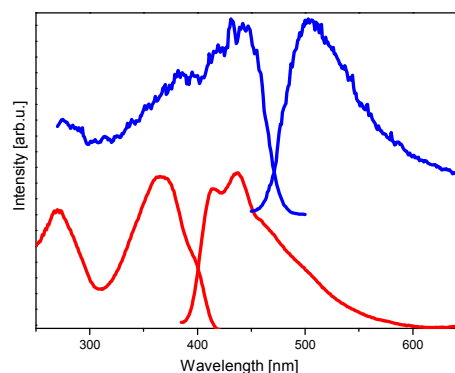


Figure 12. Excitation and emission spectra of neat **1** at r.t. (red, $\lambda_{\text{exc}} = 350$ nm, $\lambda_{\text{dec}} = 440$ nm) and 77 K (blue, $\lambda_{\text{exc}} = 400$ nm, $\lambda_{\text{dec}} = 520$ nm).

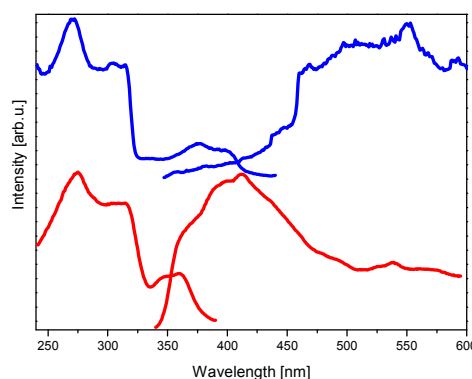


Figure 13. Excitation and emission spectra of neat **4** at r.t. (red, $\lambda_{\text{exc}} = 300$ nm, $\lambda_{\text{dec}} = 410$ nm) and 77 K (blue, $\lambda_{\text{exc}} = 320$ nm, $\lambda_{\text{dec}} = 460$ nm).

Complex **1** exhibits a structured HE band at 437 nm at r.t. and a broad emission with a long tail at 504 nm at 77 K (Figure 12). For complex **2** no authentic emission could be detected at ambient temperature. However, it is emissive at 77 K ($\lambda_{\text{em}} = 533$ nm, Figure S2). Both complexes contain a borate based ligand with an octahedrally coordinated lead ion.

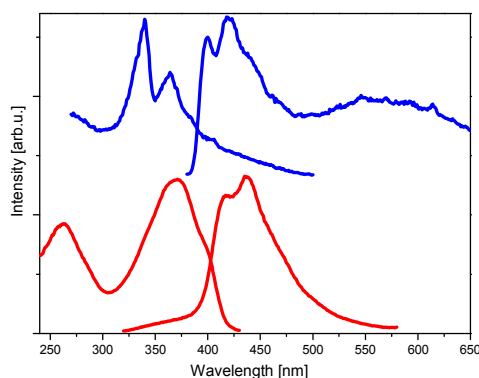


Figure 14. Excitation and emission spectra of neat **5** at r.t. (red, $\lambda_{\text{exc}} = 300$ nm, $\lambda_{\text{dec}} = 450$ nm) and 77 K (blue, $\lambda_{\text{exc}} = 360$ nm, $\lambda_{\text{dec}} = 520$ nm).

5 Complexes **3** and **4** contain a ligand which differs only in the methyl substituent. Although they have different solid state structures, they exhibit similar luminescence behaviour which is different to the other complexes presented here (Figures 13 and S10): They feature a dual emission with a more intense HE band and a less intense LE band at ambient temperature. At 77 K, the LE band is dominant. All intense bands are structured. We observed a similar behaviour when investigating gold complexes bearing aryl-substituents and assigned these emission bands to intra-ligand fluorescence and phosphorescence, respectively.⁴³

15 **Complex 5** has a structured HE band at 436 nm at room temperature and features a dual emission at 77 K with both a structured HE (419 nm) and a broad LE band (~570 nm, Figure 14). For complex **8** and **9** the solid state structures are compa-

20 rable leading to comparable emission spectra of the complexes (Figures 15 and S11). They are only slightly affected by a temperature change and show a broad LE emission bands at both ambient temperature (**8**: 493 nm; **9**: 592 nm) and
25 77 K (**8**: 488 nm; **9**: 558 nm). Complex **10** is emissive exclusively at 77 K featuring a band at ~556 nm (Figure S12).

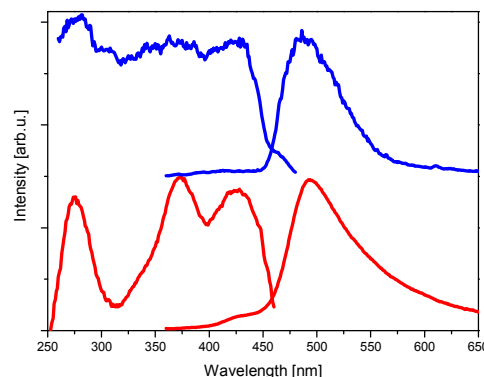


Figure 15. Excitation and emission spectra of neat **8** at r.t. (red, $\lambda_{\text{exc}} = 340$ nm, $\lambda_{\text{dec}} = 480$ nm) and 77 K (blue, $\lambda_{\text{exc}} = 340$ nm, $\lambda_{\text{dec}} = 500$ nm).

30 It can be summarized that – albeit some similarities within a subgroup of complexes are observed – no general relationship between the solid structures (coordination number and geometry, hemi- vs. holo-directed) or used ligand or its coordination mode
35 and the luminescence behaviour is obvious.

Table 8. Electronic spectroscopic data of ligands **L1** – **L5**, **L8** – **L10** and complexes **1** – **5**, **8** – **10** (unless otherwise stated, absorption spectra were measured in ethanol; emission and excitation spectra of solid samples).

| | Absorption [nm] ($\lg \epsilon$) | T [K] | Excitation [nm] | Emission [nm] |
|------------------|---|---------|-------------------------|---|
| Ligands | | | | |
| L1 | 249 (4.09), 307 (4.18) | | | |
| L2 | 234 (4.10), 317 sh (4.23) | | | |
| L3 | 219 (4.53), 247 (4.58), 295 sh (4.55), 306 (4.68) | | | |
| L4 | 221 (4.55), 250 (4.60), 302 sh (4.68), 310 (4.69) | | | |
| L5 | 252 (4.14) | | | |
| L8 | 243 (3.98), 309 (4.09) | | | |
| L9 | 246 (3.98) | | | |
| L10 | 235 (4.36), 322 (4.50) | | | |
| Complexes | | | | |
| 1 | 243 (4.26), 307 (4.36) | r.t. | 271, 367, 401 (sh) | 414, 437, 466 (sh), 498 (sh) |
| | | 77 K | 274, 386, 441 | 504 |
| 2 | 322 (4.68) ^(a) | 77 K | <450 | 533 |
| 3 | 216 (4.53), 247 (4.54), 295 (4.62), 306 (4.63) | r.t. | 264, 363 | 414, 437, 464 (sh), 602 (br) |
| | | 77 K | 396, 432 | 444, 497, 526, 552, 620 |
| 4 | 221 (5.35), 250 (5.41), 300 sh (5.49), 310 (5.50) | r.t. | 275, 314, 346, 359 | 364 (sh), 389 (sh), 398, 411, 436 (sh), 479, 490, 523, 538, 574 |
| | | 77 K | 271, 303, 314, 376, 399 | 439, 448, 468, 497, 551, 591 |
| 5 | 273 (3.36) | r.t. | 263, 370, 401 (sh) | 417, 436, |
| | | 77 K | 340, 365 | 400, 419, 439 (sh), 570 (br) |
| 8 | 314 (4.69) ^(a) | r.t. | 275, 338 (sh), 373, 425 | 428 (sh), 493 |
| | | 77 K | <445 | 488 |
| 9 | 238 (2.99), 290 (3.07), 378 (3.19) | r.t. | 324, 368, 394 | 523 (sh), 565, 592 |
| | | 77 K | 313, 354 | 558 |

10 235 (4.32), 325 (4.46)^(b)

a – dmf, b – dcm

77 K

281, 335, 368, 397

556

Conclusion

Ten new lead(II) complexes with sulphur-rich ligand environments have been synthesized and spectroscopically as well as structurally characterized. The majority of them have hemi-directed environment around their lead atoms with coordination numbers in the range 4 – 8. X-ray crystallography further revealed that most of them have extended structures (polymeric chains, double chains or sheet like structures). Complex **2a** has a BH...Pb interaction which makes it a unique example in the chemistry of lead with dipodal boron-centred soft ligands. All the complexes are almost insoluble in common organic solvents except dmf or dmsO, however, in these highly polar solvents most of them are dissociated. Despite of equal opportunity of hard and soft donor sites in the ligands L¹ – L¹⁰, the lead(II) ions exhibit affinity solely for sulphur donor sites in complexes **2**, **3**, **4** and **6** while in all other cases the metal ions coordinate both, nitrogen and sulphur donor sites, simultaneously. Most of the complexes are emissive under both ambient conditions and 77 K in the solid state. However, no obvious relationship between their solid state structures and luminescence behaviour with respect to the nature of the excited state could be identified.

Experimental work

All the solvents used during this work were dried and distilled before use. 2-mercaptobenzimidazole(L³), 2-mercapto-5-methylbenzimidazole(L⁴), 3-mercapto-1,2,4-triazole (L⁵H), 3-mercapto-4-methyl-1,2,4-triazole (L⁶), 2-mercapto-1,3,4-thiadiazole (L⁷H), 2-mercapto-5-methyl-1,3,4-thiadiazole (L⁸H), 5-mercapto-1-methyltetrazole (L⁹H), 2-mercapto-4-phenyltetrazole (L¹⁰H) and Pb(NO₃)₂ were procured from Alfa Aesar, Sigma Aldrich or Acros Organic and used without further purification. Tripodal boron substituted ligands (L¹) and dipodal boron substituted ligand (L²) were synthesised according to literature procedures.¹⁸ NMR spectra were recorded on Bruker Avance 300, Bruker DRX 500 or Bruker Avance 500 spectrometers and the chemical shifts of ¹H NMR and ¹³C NMR were referenced to the residual proton (¹H) or the carbon signals of the deuterated solvents and are reported in ppm. Elemental analyses were performed using a EuroEA Elemental Analyser. Melting points were determined using a Büchi B 545 melting point apparatus and are uncorrected. All operations were carried out in inert atmosphere of nitrogen using Schlenk and glove box techniques.

Syntheses of complexes 1–2

Ligand (L¹/L²) 0.720 mmol and lead(II) nitrate (0.360 mmol) were dissolved and stirred separately in 20 mL of THF and methanol, respectively. The solution of ligand was slowly added to that of lead(II) nitrate solution under N₂ atmosphere. The resulting solution was stirred at room temperature for 2 – 3 h and then filtered. The volume of the sample was reduced under vacuum. Yellow coloured solids were obtained, which were washed with small amounts of thf, methanol, then dried.

[PbL₂¹] **1**: Crystals suitable for diffraction were obtained by slow diffusion of *n*-pentane into a 1-methyl-2-pyrrolidinone solution of the complex [Pb(L¹)₂(L⁷H)₂L¹] (**1a**); yield 76 %; m.p. 236 – 239

°C (with decomposition). Anal. calcd. for C₆H₄BN₆PbS₆ (found): C 12.63 (12.85), H 0.71 (1.04), N 14.73 (14.75), S 33.72 (34.90). ¹H NMR (dmf-d7) δ = 8.07 (s, 6H, HC=N), ¹H NMR (dmsO-d6) δ = 8.54 (s, 6H, HC=N), ¹³C NMR (dmsO-d6) δ = 189.2 (C=S), 144.4 (C=N).

Free ligand compound (L¹): ¹H NMR (dmsO-d6) δ = 8.57 (s, 3H, HC=N); ¹³C NMR (dmsO-d6) δ = 189.3 (C=S), 145.4 (C=N); ¹¹B NMR (dmsO-d6) δ = –2.36 ppm.

[PbL₂²] **2**: Crystals were obtained by slow evaporation of a dmf solution of complex **2**; yield 81 %; m.p. 247 °C (with decomposition). Anal. calcd. for C₁₆H₂₀B₂N₄PbS₈ (found): C 20.00 (20.72), H 2.10 (1.75), N 5.83 (5.98). ¹H NMR (dmsO-d6) δ = 6.34 (s, 4H, HC=N), not observed (BH₂), 2.13 (s, 12H, H₃C); ¹³C NMR (dmsO-d6) δ = 175.9 (C=S), 149.6 (C=N), 109.8 (C-CH₃), 17.0 (H₃C); ¹¹B NMR (dmsO-d6) δ = –14.1, –1.76 ppm; ²⁰⁷Pb NMR (dmf-d7) δ = –461 ppm.

Free ligand compound (L²): ¹H NMR (dmsO-d6), δ = 6.22, (s, 2H, HC-ring), 3.17 (br, 2, BH₂), 2.37 (s, 6H, CH₃); ¹³C NMR (dmsO-d6), δ = 189.9 (C=S), 147.7 (C=N), 105.4 (C-CH₃), 19.2 (CH₃); ¹¹B NMR = –11.25 ppm.

Syntheses of complexes 3 – 6 and 9 – 10

Solution of the heterocyclic ligands L³, L⁴, L⁵H, L⁶, L⁹H and L¹⁰H (4.00 mmol) in 10 mL of THF was added drop-wise to a solution of lead(II) nitrate (2.00 mmol) in 10 mL of dmf, stirred at room temperature and finally heated to 90 °C for 3 – 4 h. The resulting clear solutions were concentrated under vacuum resulting precipitation. The precipitates were filtered off, washed with small amounts of THF, then with acetone and finally dried.

[PbL₂³(NO₃)₂] **3**: Single crystals were obtained by slow cooling of a warm solution of complex **3** in dmf/methanol; yield 78 %; m.p. 190 °C. Anal. calcd. for C₁₄H₁₂N₆O₆PbS₂ (found): C 26.62 (27.09), H 1.91 (1.90), N 13.31 (13.15), S 10.15 (10.69). ¹H NMR (dmsO-d6) δ = 11.52 (s, 4, NH), 7.11 – 7.16 (m, 8H, H₅C₆-ring); ¹³C NMR (dmsO-d6) δ = 168.5 (C7), 132.7 (C1, C6), 122.7 (C2, C5), 109.8 (C3, C4).

Free ligand compound (L³): ¹H NMR (dmsO-d6) δ = 12.52 (s, 1, NH), 7.09 – 7.16 (m, 4H, H₅C₆-ring); ¹³C NMR (dmsO-d6) δ = 168.6 (C7), 132.7 (C1, C6), 122.8 (C2, C5), 110.0 (C3, C4).

[PbL₃⁴(μ-L⁴)(NO₃)₂] **4**: Single crystals were obtained by slowly cooling of a warm solution of complex **4** in dmf/thf; yield 65 %; m.p. 226 – 229 °C (with decomposition). Anal. calcd. for C₇₂H₈₀N₂₀O₁₆Pb₂S₈ (found): C 40.18 (39.65), H 3.75 (3.80), N 13.01 (13.01), S 11.92 (11.99). ¹H NMR (dmsO-d6) δ = 12.40 (s, 2, NH), 6.91 – 7.06 (m, 4H, H₅C₆-ring), 2.33 (s, 3H, CH₃); ¹³C NMR (dmsO-d6) δ = ¹³C NMR (dmsO-d6) δ = 168.2 (C8), 133.0 (C1), 132.0 (C6), 130.7 (C2), 123.5 (C5), 110.1(C3), 109.6 (C4), 21.4 (C7).

Free ligand compound (L⁴): ¹H NMR (dmsO-d6) δ = 12.40 (s, 2, NH), 6.92 – 7.06 (m, 4H, H₅C₆-ring), 2.33 (s, 3H, CH₃); ¹³C NMR (dmsO-d6) δ = 168.2 (C8), 132.7 (C1), 132.0 (C6), 130.6 (C2), 123.5 (C5), 110.1 (C3), 109.6 (C4), 21.4 (C7).

[Pb(L⁵)(L⁵H)₂(NO₃)(H₂O)] **5**: Single crystals were obtained by cooling the solution of complex **5** in dmf/thf in a refrigerator; yield 74 %; m.p. 207 – 210 °C (with decomposition). Anal. calcd. for C₆H₅N₁₀O₄PbS₃ (found): C 12.33 (12.50), H 0.86 (1.49), N 23.96 (24.10), S 16.46 (16.88). ¹H NMR (dmsO-d6) δ = 14.12 (br,

2H, NH), 8.56 (s, 1H, HC=N); ^{13}C NMR = 156.6 (C=S), 147.0 (C=N).

Free ligand compound (L⁵H): ^1H NMR (dmsO-d6) δ = 13.38 (br, 2H, NH), 8.25 (s, 1H, HC=N); DMSO-d6 δ = 166.0 (C=S), 141.0 (C=N).

$[\text{PbL}_4(\text{NO}_3)_2]_n$ **6**: Single crystals were obtained by cooling the solution of complex **6** in dmf/thf in refrigerator; yield 87 %; m.p. 140 – 142 °C (with decomposition). Anal. calcd. for $\text{C}_{12}\text{H}_{20}\text{N}_{14}\text{O}_6\text{PbS}_4$ (found): C 18.20 (17.94), H 2.55 (2.60), N 24.76 (24.92); S 16.20 (16.64). ^1H NMR (dmsO-d6) δ = 13.66 (br, 4H, NH), 8.42 (s, 4H, CH), 3.43 (s, 12H, H₃C); ^{13}C NMR (dmsO-d6) δ = 166.6 (C=S), 143.3 (C=N), 31.7 (H₃C).

Free ligand compound (L⁶): ^1H NMR (dmsO-d6) δ C= 13.63 (s, 1H, NH) 8.39 (s, 1H, HC=N), 3.43 (s, 3H, H₃C); ^{13}C NMR (dmsO-d6) δ = 166.7 (C=S), 143.1 (C=N), 31.7 (H₃C).

$[\text{PbL}_2\text{H}]_n$ **9**: Single crystals were obtained by low evaporation of the solution of complex **9** in dmf/thf; yield 87 %; m.p. 203 – 206 °C (with decomposition). Anal. calcd. for $\text{C}_4\text{H}_6\text{N}_8\text{PbS}_2$ (found): C 10.98 (11.01), H 1.38 (1.32), N 25.61 (25.09). ^1H NMR (dmsO-d6) δ = 3.76 (s, 3H, H₃C), ^{13}C NMR (dmsO-d6) δ = 161.7 (C=S), 33.5 (H₃C), ^{207}Pb NMR (dmf-d7) δ = -2628 ppm.

Free ligand compound L⁹H: ^1H NMR (dmsO-d6) δ = 3.78 (s, 3H, H₃C-), ^{13}C NMR (dmsO-d6) δ = 164.6 (C=S), 33.8 (H₃C).

$[\text{PbL}^{10}_2\text{H}]_n$ **10**: Single crystals were obtained by slow evaporation of a solution of complex **10** in dmf/thf; yield 87 %; m.p. 266 – 269 °C (with decomposition). Anal. calcd. for $\text{C}_{18}\text{H}_{12}\text{N}_2\text{PbS}_4$ (found): C 36.53 (37.35), H 2.10 (2.57), N 4.73 (6.05), S 21.67 (21.69). ^1H NMR (dmsO-d6) δ = 7.83 – 7.86 (dd, 2H, C2H, C6H), 7.23 – 7.37 (m, 3H, C3H–C5H), overlap in aryl region (CH–thiazole ring); ^{13}C NMR (dmsO-d6) δ = not measured due to limited solubility.

Free ligand compound (L¹⁰H): ^1H NMR (dmsO-d6) δ = 13.66 (br, 1H, NH), 7.75 – 7.77 (dd, 2H, C2H, C6H), 7.40 – 7.48 (m, 3H, C3H–C5H), 7.32 (CH–thiazole ring).

Synthesis of complexes 7 and 8

Compounds **7** and **8** were synthesized and crystallized by the branched tube method: 1.0 mmol of heterocyclic ligand (L⁷H or L⁸H) and 0.5 mmol of lead(II) nitrate were placed in a separate arm of a branched tube. Methanol was then carefully added under N₂ atmosphere to fill both arms. The tube was stoppered and the ligand-containing arm was immersed in a bath held at 55 °C, while the other was left at room temperature. After 2 d, crystals were formed in the room temperature arm. These crystals were then filtered off, washed with acetone, dried and stored under an atmosphere of N₂.

$[\text{Pb}(\text{L}^7)_2(\text{L}^7\text{H})(\text{CH}_3\text{OH})]_n$ **7**: Single crystals for this complex were obtained by the branched tube method; yield 76 %; m.p. 196 – 198 °C (with decomposition). Anal. calcd. for $\text{C}_9\text{H}_7\text{N}_8\text{OPb}_2\text{S}_8$ (found): C 11.83 (11.72), H 0.77 (0.76), N 12.26 (12.69), S 28.06 (27.38). ^1H NMR (dmsO-d6) δ = 8.91 (s, 4H, HC=N); ^{13}C NMR (dmsO-d6) δ = not observed (C=S), 150.3 (C=N); ^{207}Pb NMR (dmf-d7) δ = -2811 ppm.

Free ligand compound (L⁷H): ^1H NMR (dmsO-d6) δ = 14.63 (s, 1H, NH), 8.87 (s, 1H, HC=N); ^{13}C NMR (dmsO-d6) δ = 188.2 (C=S), 150.1 (C=N).

$[\text{PbL}^8_2\text{H}(\text{NO}_3)_2]_n$ **8**: Single crystals for this complex were obtained by the branched tube method; yield 69 %; m.p. 238 – 240 °C (with decomposition). Anal. calcd. for $\text{C}_{12}\text{H}_{16}\text{N}_8\text{S}_8\text{Pb}$ (found): C 19.58 (19.31), H 2.19 (1.97), N 15.22 (14.93), S 34.85 (33.77). ^1H NMR (dmsO-d6) δ = 2.55 (s, 3H, CH₃), ^{13}C NMR (dmsO-d6) δ = 190.1 (C=S), 154.3 (C=N), 16.4 (CH₃); ^{207}Pb NMR (dmf-d7) δ = -2585 ppm.

Free ligand compound (L⁸H): ^1H NMR (dmsO-d6) δ = 2.45 (s, 3H, CH₃), ^{13}C NMR (dmsO-d6) δ = 189.2 (C=S), 160.1 (C=N), 16.2 (CH₃).

Photophysical Characterisation. Spectroscopic-grade solvents were used for all photophysical characterizations. Absorption spectra were recorded with a Varian Cary 300 double-beam spectrometer. Emission spectra at 300 and 77 K were recorded with a Jobin-Yvon Fluorolog 3 steady-state fluorescence spectrometer. The estimated experimental errors are 5% in the molar absorption coefficients.

X-Ray diffraction experiments. X-ray diffraction data were collected from single crystals of **1a**, **2**, **3**, **4**, **5**, **6**, **7**, **8**, **9** and **10**. Crystals suitable for X-ray diffraction were picked under inert paratone oil, mounted on a glass fibre and transferred onto the goniometer of the diffractometer into a cold gas stream. Data for **3**, **4**, **6** and **7** were collected on a Bruker Nonius Kappa CCD diffractometer with radiation source Mo-K α , while data for compounds **1a** (with Mo-K α radiation source) and **5** (with Cu-K α radiation source) were collected using Bruker AXS Kappa with APEX II. Similarly crystal data of complexes **2**, **8**, **9** and **10** (all with Mo-K α except **2** with Cu radiation source) were collected using Super Nova, Dual, Atlas diffractometer. A summary of data collections and structure refinements is reported in Tables 9 and 10. The structures were solved by direct methods and refined by full-matrix least squares cycles (programs SHELXS-97 or SHELXL-97)⁴⁴ and Olex2.⁴⁵

Cite this: DOI: 10.1039/c0xx00000x

www.rsc.org/xxxxxx

ARTICLE TYPE

Table 9. X-ray crystallographic data for compounds 1 – 5

| Compound | 1a | 2 | 3 | 4 | 5 |
|--|---|--|--|--|---|
| Empirical formula | C ₁₃ H ₁₄ BN ₉ OPbS ₈ | C ₁₆ H ₂₀ B ₂ N ₄ PbS ₈ | C ₁₄ H ₁₂ N ₆ O ₆ PbS ₂ | C ₇₂ H ₈₀ N ₂₀ O ₁₆ Pb ₂ S ₈ | C ₂ H ₄ N ₄ O ₄ PbS |
| <i>M_r</i> | 786.81 | 753.65 | 631.61 | 2152.42 | 387.34 |
| <i>T</i> (K) | 100(2) K | 100(2) K | 100(2) K | 100(2) K | 100(2) K |
| Crystal system | triclinic | triclinic | orthorhombic | monoclinic | orthorhombic |
| Space group | <i>P</i> $\bar{1}$ | <i>P</i> $\bar{1}$ | <i>Pccn</i> | <i>C2/c</i> | <i>Pben</i> |
| <i>a</i> (Å) | 10.1258(9) | 9.93379(19) | 12.354(5) | 25.8252(2) | 17.9942(7) |
| <i>b</i> (Å) | 11.5049(11) | 12.2627(3) | 16.814(6) | 20.7570(2) | 6.3605(2) |
| <i>c</i> (Å) | 12.7990(19) | 12.4372(3) | 9.0073(18) | 15.8960(2) | 13.1333(5) |
| α (°) | 111.827(6) | 65.316(2) | 90 | 90 | 90 |
| β (°) | 108.210(6) | 83.1389(17) | 90 | 90.0600(6) | 90 |
| γ (°) | 95.805(5) | 66.8959(19) | 90 | 90 | 90 |
| <i>Z</i> | 2 | 2 | 4 | 4 | 8 |
| <i>V</i> (Å ³) | 1274.3(3) | 1264.40(5) | 1870.9(11) | 8521.10(15) | 1503.13(9) |
| <i>F</i> (000) | 756 | 728 | 1200 | 4288 | 1392 |
| Cryst. size (mm) | 0.38 × 0.24 × 0.14 | 0.35 × 0.21 × 0.15 | 0.30 × 0.09 × 0.03 | 0.26 × 0.14 × 0.10 | 0.33 × 0.05 × 0.03 |
| Refl. measured | 87623 | 74818 | 19912 | 163344 | 27266 |
| Unique refl. (<i>R_{int}</i>) | 7414(0.0263) | 7372(0.0459) | 2139(0.0662) | 12428(0.077) | 1418(0.0453) |
| No. of param. | 293 | 300 | 132 | 566 | 122 |
| <i>R</i> (<i>I</i> > 2σ(<i>I</i>)) | 0.0150 | 0.0146 | 0.0270 | 0.0319 | 0.0195 |
| <i>R_w</i> (all refl.) | 0.0356 | 0.0327 | 0.0515 | 0.0825 | 0.0553 |
| Goodness-of-fit | 1.047 | 1.085 | 1.016 | 1.039 | 1.195 |
| $\rho_{\text{max/min}}$ (e Å ⁻³) | 1.33/−1.17 | 0.52/−0.70 | 2.45/−0.68 | 1.78/−0.66 | 1.36/−0.84 |
| CCDC no. | 992111 | 992112 | 992113 | 1008780 | 992115 |

Table 10. X-ray crystallographic data for compounds 6 – 10

| Compound | 6 | 7 | 8 | 9 | 10 |
|--|---|--|--|---|---|
| Empirical formula | C ₁₂ H ₂₀ N ₁₄ O ₆ PbS ₄ | C ₉ H ₇ N ₈ OPb ₂ S ₈ | C ₆ H ₆ N ₄ S ₄ Pb | C ₄ H ₆ N ₈ PbS ₂ | C ₁₈ H ₁₂ N ₂ PbS ₄ |
| <i>M_r</i> | 791.85 | 914.09 | 469.58 | 437.48 | 591.73 |
| <i>T</i> (K) | 100(2) K | 100(2) K | 100(2) K | 100(2) K | 100(2) K |
| Crystal system | tetragonal | monoclinic | monoclinic | monoclinic | orthorhombic |
| Space group | <i>I</i> $\bar{4}$ | <i>P2</i> ₁ | <i>P2</i> ₁ / <i>c</i> | <i>P2</i> ₁ / <i>n</i> | <i>Pbca</i> |
| <i>a</i> (Å) | 10.5430(11) | 4.0517(1) | 13.3192(4) | 8.94447(19) | 19.9345(3) |
| <i>b</i> (Å) | 10.5430(11) | 24.3412(7) | 11.7420(4) | 4.92209(8) | 7.34785(13) |
| <i>c</i> (Å) | 11.7670(6) | 10.7681(4) | 7.72600(19) | 23.5863(5) | 24.3982(4) |
| α (°) | 90 | 90 | 90 | 90 | 90 |
| β (°) | 90 | 93.9769(17) | 93.931(2) | 92.5552(18) | 90 |
| γ (°) | 90 | 90 | 90 | 90 | 90 |
| <i>Z</i> | 2 | 2 | 4 | 4 | 8 |
| <i>V</i> (Å ³) | 1308.0(3) | 1059.43(6) | 1205.46(6) | 1037.36(4) | 3573.75(11) |
| <i>F</i> (000) | 768 | 834 | 864 | 800 | 2240 |
| Cryst. size (mm) | 0.30 × 0.28 × 0.28 | 0.20 × 0.03 × 0.03 | 0.20 × 0.06 × 0.02 | 0.49 × 0.09 × 0.03 | 0.18 × 0.05 × 0.04 |
| Refl. measured | 13152 | 22633 | 44530 | 77856 | 31790 |
| Unique refl. (<i>R_{int}</i>) | 1804(0.0373) | 4808(0.097) | 4649(0.0392) | 1819(0.0894) | 3150(0.0370) |
| No. of param. | 105 | 254 | 139 | 138 | 226 |
| <i>R</i> (<i>I</i> > 2σ(<i>I</i>)) | 0.0130 | 0.0386 | 0.0404 | 0.0357 | 0.0208 |
| <i>R_w</i> (all refl.) | 0.0284 | 0.0964 | 0.1131 | 0.0943 | 0.0444 |
| Goodness-of-fit | 0.965 | 1.013 | 1.095 | 1.121 | 1.187 |
| $\rho_{\text{max/min}}$ (e Å ⁻³) | 0.78/−0.74 | 2.18/−2.08 | 1.48/−1.80 | 3.32/−3.08 | 0.78/−0.68 |
| CCDC no. | 992116 | 992117 | 992118 | 992119 | 992120 |

Cite this: DOI: 10.1039/c0xx00000x

www.rsc.org/xxxxxx

ARTICLE TYPE

Notes and references

- ^a Universität Bielefeld, Lehrstuhl für Anorganische Chemie und Strukturchemie, Centrum für Molekulare Materialien CM₃, Universitätsstraße 25, 33615 Bielefeld, Germany, Tel. +44 521 106 6182, Fax +44 521 106 6026, E-mail: mitzel@uni-bielefeld.de
- ^b Johannes Kepler University Linz, Institut für Anorganische Chemie, Altenbergerstraße 69, 4040 Linz, Austria, Tel. +43 732 2468 8801, Fax +43 732 2468 968, E-mail: Uwe.Monkowitz@jku.at
1. R. G. Pearson, *Inorg. Chem.* 1998, **27**, 734.
 2. M. Kaupp and P. v. R. Schleyer, *J. Am. Chem. Soc.* 1993, **115**, 1061.
 3. H. Needleman, *Annu. Rev. Med.* 2004, **55**, 209.
 4. D. T. Wigle, T. E. Arbuckle, M. Walker, M. G. Wade, S. L. Liu and D. Krewski, *J. Toxicol. Environ. Health. Part B* 2007, **10**, 3.
 5. A. B. Ghering, L. M. M. Jenkins, B. L. Schenck, S. Deo, R. A. Mayer, M. J. Pikaart, J. G. Omichinski and H. A. Godwin, *J. Am. Chem. Soc.* 2005, **127**, 3751.
 6. J. M. Berg and H. A. Godwin, *Annu. Rev. Biophys. Biomol. Struct.* 1997, **26**, 357.
 7. R. L. Davidovich, V. Stavila and K. H. Whitmire, *Coord. Chem. Rev.* 2010, **254**, 2193.
 8. C. E. Holloway and M. Melnik, *Main Group Met. Chem.* 1997, **20**, 399.
 9. J. Parr, *Polyhedron*, 1997, **16**, 551.
 10. J. Parr, Germanium, Tin, and Lead; in *Comprehensive Coordination Chemistry II*, vol. 3, Elsevier, Oxford, 2004, pp. 545.
 11. S. Hino, M. Brynda, A. D. Phillips and P. P. Power, *Angew. Chem.* 2004, **116**, 2706; *Angew. Chem. Int. Ed.* 2004, **43**, 2655.
 12. (a) Y. C. Zhang, T. Qiao, X. Y. Hu, G. Y. Wang and X. Wu, *J. Cryst. Growth* 2005, **277**, 518; (b) M. Afzaal, K. Ellwood, N. L. Pickett, P. O'Brien, J. Raftery and J. Waters, *J. Mater. Chem.* 2004, **14**, 1310; (c) P. Boudjouk, B. R. Jarabek, D. L. Simonson, D. J. Seidler, D. G. Grier, G. J. McCarthy and L. P. Keller, *Chem. Mater.* 1998, **10**, 2358; (d) G. Zhou, M. Lü, Z. Xiu, S. Wang, H. Zhang, Y. Zhou, S. Wang, *J. Phys. Chem. B* 2006, **110**, 6543.
 13. R. D. Hancock and A. E. Martell, *Chem. Rev.* 1989, **89**, 1875.
 14. L. Shimoni-Livny, J. P. Glusker and C. W. Bock, *Inorg. Chem.* 1998, **37**, 1853.
 15. M. Imran, B. Neumann, H.-G. Stammler, U. Monkowitz, M. Ertl and N. W. Mitzel, *Dalton Trans.* 2013, **42**, 15785.
 16. M. Imran, B. Neumann, H.-G. Stammler, U. Monkowitz, M. Ertl and N. W. Mitzel, *Dalton Trans.* 2014, **43**, 1267.
 17. (a) M. A. Baldo, S. Lamansky, P. E. Burrows, M. E. Thompson and S. R. Forrest, *Appl. Phys. Lett.*, 1999, **75**, 4. (b) C. Adachi, M. A. Baldo, S. R. Forrest and M. E. Thompson, *Appl. Phys. Lett.*, 2000, **77**, 904. (c) M. Ikai, S. Tokito, Y. Sakamoto, T. Suzuki and Y. Taga, *Appl. Phys. Lett.* 2001, **79**, 156. (d) R. J. F. Berger, B. Neumann, H.-G. Stammler and N. W. Mitzel, *Eur. J. Inorg. Chem.* 2010, 1613.
 18. R. M. Silva, C. Gwengo, S. V. Lindeman, M. D. Smith and J. R. Gardinier, *Inorg. Chem.* 2006, **45**, 10998.
 19. (a) B. M. Bridgewater and G. Parkin, *Inorg. Chem. Commun.* 2000, **3**, 534; (b) Brian M. Bridgewater and Gerard Parkin, *J. Am. Chem. Soc.* 2000, **122**, 7140.
 20. C. Kimblin, B. M. Bridgewater, T. Hascall and G. Parkin, *J. Chem. Soc., Dalton Trans.* 2000, 891.
 21. J. Reglinski, M. D. Spicer, M. Garner and A. R. Kennedy, *J. Am. Chem. Soc.* 1999, **121**, 2317.
 22. P. A. Slavin, J. Reglinski, M. D. Spicer and A. R. Kennedy, *J. Chem. Soc., Dalton Trans.* 2000, 239.
 23. C. A. Dodds, J. Reglinski and M. D. Spicer, *Chem.–Eur. J.* 2006, **12**, 931.
 24. J. Reglinski, M. D. Spicer, M. Garner and A. R. Kennedy, *J. Am. Chem. Soc.* 1999, **121**, 2317.
 25. J. R. Gardinier, R. M. Silva, C. Gwengo and S. V. Lindeman, *Chem. Commun.* 2007, 1524.
 26. C. Kimblin, B. M. Bridgewater, T. Hascall and G. Parkin, *J. Chem. Soc., Dalton Trans.* 2000, 1267.
 27. N. Tsoureas, G. R. Owen, A. Hamilton and A. G. Orpen, *Dalton Trans.* 2008, **43**, 6039.
 28. G. Dyson, A. Hamilton, B. Mitchell and G. R. Owen, *Dalton Trans.* 2009, **31**, 6120.
 29. Y. Z. Yuan, J. Zhou, X. Liu, L. H. Liu and K. B. Yu, *Inorg. Chem. Commun.* 2007, **10**, 475.
 30. S. Bristow and J. A. Harrison, *Polyhedron* 1987, **6**, 2177.
 31. F. Marandi and H. Krautscheid, *Z. Naturforsch.* 2009, **64b**, 1027.
 32. A. Bondi, *J. Phys. Chem.* 1964, **68**, 441.
 33. J. S. Magyar, T. S. Weng, C. M. Stern, D. F. Dye, B. W. Rous, J. C. Payne, B. M. Bridgewater, A. Mijovilovich, G. Parkin, J. M. Zaleski, J. E. Penner-Hahn and H. A. Godwin, *J. Am. Chem. Soc.* 2005, **127**, 9495.
 34. J. K. Cheng, J. Zhang, P. X. Yin, Q. P. Lin, Z. J. Li and Y. G. Yao, *Inorg. Chem.* 2009, **48**, 9992.
 35. Q.Y. Li, G. W. Yang, Y. S. Ma, M. J. Li, Y. Zhou, *Inorg. Chem. Commun.* 2008, **11**, 795.
 36. (a) J. Y. Sun, L. Wang, D. J. Zhang, D. Li, Y. Cao, L. Y. Zhang, S. L. Zeng, G. S. Pang, Y. Fan, J. N. Xu and T. Y. Songa, *Cryst. Eng. Commun.* 2013, **15**, 3402; (b) L. S. Jie, S. W. Dong, M. D. Liang, M. D. Yun, Chin. *J. Struct. Chem.* 2011, **30**, 1049; (c) R. R. Zhuang, F. F. Jian, K. F. Wang, *Turk. J. Chem.* 2010, **34**, 571.
 37. G. Nuss, G. Saischek, B. N. Harum, M. Volpe, K. Gatterer, F. Belaj and N. C. Mösch-Zanetti, *Inorg. Chem.* 2011, **50**, 1991.
 38. R. J. F. Berger, D. Rettenwander, S. Spirk, C. Wolf, M. Patzschke, M. Ertl, U. Monkowitz and N. W. Mitzel, *Phys. Chem. Chem. Phys.* 2012, **14**, 15520.
 39. A. Vogler, H. Nikol, *Pure Appl. Chem.* 1992, **64**, 1311.
 40. K. Oldenburg, A. Vogler, I. Mikó, O. Horváth, *Inorg. Chim. Acta* 1996, **248**, 107.
 41. (a) A. Strasser, A. Vogler, *J. Photochem. Photobiol. A* 2004, **165**, 115; (b) A. Strasser, A. Vogler, *Inorg. Chem. Commun.* 2004, **7**, 528.
 42. (a) K.-L. Zhang, F. Zhou, R. Wu, B. Yang, S. W. Ng, *Inorg. Chim. Acta* 2009, **362**, 4255; (b) J. He, M. Zeller, A. D. Hunter, Z. Xu, *J. Am. Chem. Soc.* 2012, **134**, 1553; (c) A. C. Wibowo, S. A. Vaughn, M. D. Smith, H.-C. zur Loye, *Inorg. Chem.* 2010, **49**, 11001; (d) Y.-H. Zhao, H.-B. Xu, Y.-M. Fu, K.-Z. Shao, S.-Y. Yang, Z.-M. Su, X.-R. Hao, D.-X. Zhu, E.-B. Wang, *Cryst. Growth Des.* 2008, **8**, 3566; (e) L. Zhang, Z.-J. Li, Q.-P. Lin, Y.-Y. Qin, J. Zhang, P.-X. Yin, J.-K. Cheng, Y.-G. Yao, *Inorg. Chem.* 2009, **48**, 6517; (f) E.-C. Yang, J. Li, B. Ding, Q.-Q. Liang, X.-G. Wang and X.-J. Zhao, *CrystEngComm* 2008, **10**, 158; (g) Q.-Y. Liu and L. Xu, *Eur. J. Inorg. Chem.* 2006, 1620; (h) J. Yang, G.-D. Li, J.-J. Cao, Q. Yue, G.-H. Li and J.-S. Chen, *Chem. Eur. J.* 2007, **13**, 3248.
 43. (a) M. Kriechbaum, M. List, R. J. F. Berger, M. Patzschke and U. Monkowitz, *Chem. Eur. J.* 2012, **18**, 5506; (b) M. Kriechbaum, G. Winterleitner, A. Gerisch, M. List and U. Monkowitz, *Eur. J. Inorg. Chem.* 2013, 5567; (c) M. Kriechbaum, D. Otte, M. List and U. Monkowitz, *Dalton Trans.* DOI: 10.1039/C4DT00695J..
 44. SHELXL-96, Program for Refinement of Structures, G. M. Sheldrick, *Acta Crystallogr. Sect. A* 2008, **64**, 112.
 45. O. V. Dolomanov, L. J. Bourhis, R. J. Gildea, J. A. K. Howard and H. Puschmann, *J. Appl. Crystallogr.* 2009, **42**, 339.

Cite this: DOI: 10.1039/c0xx00000x

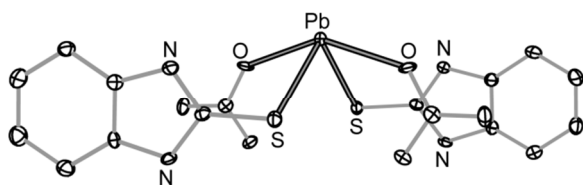
www.rsc.org/xxxxxx

ARTICLE TYPE

TOC entry

Hemi- and holo-directed lead(II) complexes in soft ligand environment

⁵ M. Imran, A. Mix, B. Neumann, H.-G. Stammler, U. Monkowski, P. Gründlinger and N. W. Mitzel*



¹⁰ Structures and stereochemical activity of the lone pairs at the lead ion were investigated by synthetic, spectroscopic and structural studies of ten lead(II) complexes with heterocyclic soft ligands. The majority of the complexes exhibited hemi-directed environment around lead ions.

¹⁵